PHYSICAL REVIEW B **93**, 121107(R) (2016)

Splitting between bright and dark excitons in transition metal dichalcogenide monolayers

J. P. Echeverry, B. Urbaszek, T. Amand, X. Marie, and I. C. Gerber*

Université Fédérale de Toulouse Midi Pyrénées, INSA-CNRS-UPS, LPCNO, 135 Avenue de Rangueil, 31077 Toulouse, France

(Received 27 January 2016; revised manuscript received 1 March 2016; published 16 March 2016)

The optical properties of transition metal dichalcogenide monolayers such as the two-dimensional semiconductors MoS_2 and WSe_2 are dominated by excitons, Coulomb bound electron-hole pairs. The light emission yield depends on whether the electron-hole transitions are optically allowed (bright) or forbidden (dark). By solving the Bethe-Salpeter equation on top of GW wave functions in density functional theory calculations, we determine the sign and amplitude of the splitting between bright and dark exciton states. We evaluate the influence of the spin-orbit coupling on the optical spectra and clearly demonstrate the strong impact of the intra-valley Coulomb exchange term on the dark-bright exciton fine structure splitting.

DOI: 10.1103/PhysRevB.93.121107

Introduction. Transition metal dichalcogenide (TMDC) monolayers (MLs), with chemical formula MX_2, with M=Mo or W and X = S, Se, or Te, are semiconductors with a direct band gap in the visible region situated at the K point of the Brillouin zone [1,2]. In these two-dimensional (2D) systems the broken inversion symmetry of the crystal lattice allows for optical control of the valley degrees of freedom [3–6]. Combined with strong spin-orbit coupling (SOC) this leads to valley-spin locking [7], thus opening exciting avenues for original applications in optoelectronics and spintronics. Tightly bound excitons [8–11], with binding energies around 0.5 eV, originate from the direct term of the electron-hole (e-h) Coulomb interaction, enhanced by the strong 2D quantum confinement, the large effective masses, and the reduced dielectric screening in 2D systems. While the energy spectra of these excitons have been intensively studied by combining both experimental and theoretical techniques in the last few years [12–17], little is known about their fine structure.

For optoelectronics based on TMDC MLs it is important to clarify if the lowest energy transition is optically bright or optically dark (i.e., spin forbidden) [18]. This bright-dark exciton fine-structure splitting governs the optical properties also of 2D semiconductor nanostructures such as III-V and II-VI quantum wells [19–23] as well as CdSe nanocrystals [24]. In particular, the measured low photo- or electroluminescence yield and its increase with the temperature in monolayer WSe_2 has been interpreted recently in terms of dark excitons lying at lower energy compared to the bright ones [25–29]. This will also affect the efficiency of recently demonstrated WSe_2 or WS_2 light-emitting devices [30,31]. For fundamental physics experiments an optically dark ground state can be an advantage, as it allows the study of exciton quantum fluids in Bose-Einstein exciton condensates [32]. It is thus crucial to determine both the amplitude and sign of this bright-dark exciton splitting in TMDC MLs.

Figure 1(b) presents the schematics of a typical TMDC ML band structure in a single-particle picture. In addition to the large spin-orbit splitting Δ_v between A and B *valence bands* (VBs), the interplay between inversion asymmetry and spin-orbit interaction also yields a smaller spin-splitting (Δ_c) between the lowest energy *conduction bands* (CBs) [33–36]. First let us consider A excitons, with the transitions involving only the highest VB energy (A) and the two lowest CBs ($\uparrow$ or $\downarrow$), see Fig. 1(a). Here $\Omega_{\uparrow\downarrow}$ represents dark (spin forbidden) transitions, and $\Omega_{\uparrow\uparrow}$ shows bright transitions. As a first approximation, one could consider that the energy splitting $\Delta_{\text{dark}-\text{bright}} = \Omega_{\uparrow\downarrow} - \Omega_{\uparrow\uparrow}$ between bright and dark excitons is mainly due to the CB splitting $\Delta_c = E_{\text{CB}\downarrow} - E_{\text{CB}\uparrow}$ induced by SOC. Depending on the material, Δ_c can either be negative for WX_2 or positive for MoX_2 systems (X=S, Se), as standard density functional theory (DFT) and tight-binding calculations have shown [33,34,37–40]. However, this single-particle approach misses a key ingredient for the accurate determination of the dark-bright exciton splitting: the short-range part of the e-h Coulomb exchange interaction for the exciton [19,21,41]. So far in the context of TMDC MLs, only the effects of the long-range exciton exchange interaction on the valley dynamics of bright exciton states in TMDC monolayers have been studied [42–45].

Here we demonstrate that the e-h exchange interaction within the exciton causes a splitting between the low-energy optically bright and dark excitons in TMDC MLs. We find a giant exchange term of the order of 20 meV, more than 100 times larger than in GaAs quantum wells, for instance [19,21,41]. For all the investigated MoX_2 and WX_2 MLs, this local field effect due to the exchange interaction is added algebraically to the CB spin-orbit term Δ_c, yielding a splitting $\Delta_{\text{dark}-\text{bright}}$ between bright and dark exciton that differs significantly from Δ_c, see comparison in Figure 1(a). We find that for MoX_2 systems, A-exciton dark states are higher in energy than bright ones, whereas this order is reversed for WX_2 MLs. Interestingly for the WSe_2 ML we obtain $\Delta_{\text{dark}-\text{bright}} = -16$ meV, a value in good agreement with a first experimentally derived value [28]. Importantly, we also report results on the exciton states involving the B valence band, which are fully consistent when compared to $\Delta_{\text{dark}-\text{bright}}$ for the A exciton, since the conduction band splitting contributes with the opposite sign. Moreover we show that the determination of the CB spin-orbit splitting Δ_c requires us to perform DFT-based calculations within the GW approach [46,47]. Significant changes compared to standard DFT level calculations [12,13,33,39] are obtained for all TMDC MLs.

Computational details. The atomic structures, quasiparticle band structures, and optical spectra are obtained from DFT calculations using the VASP package [48,49]. The

*igerber@insa-toulouse.fr

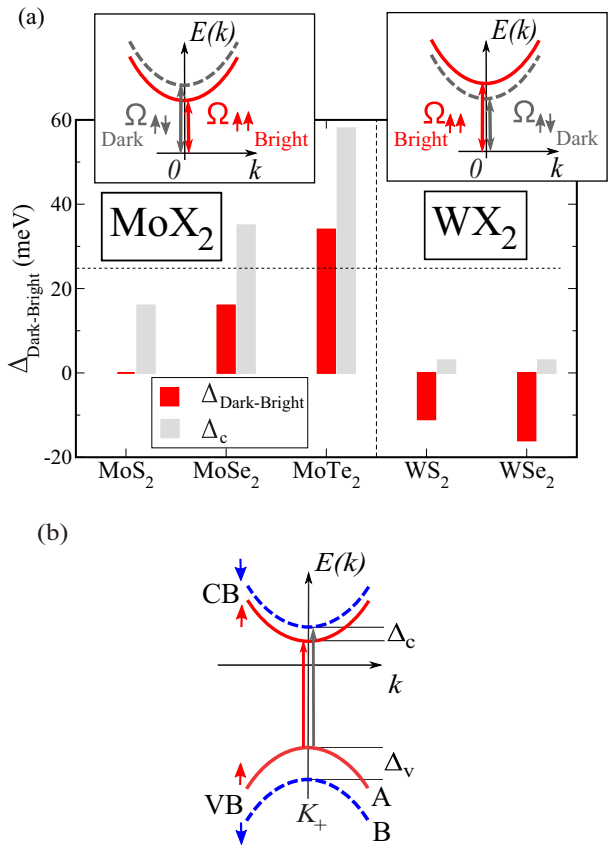

FIG. 1. (a) Dark-bright energy splittings of the A $1s$ state excitons in the MoX_2 and WX_2 systems at G_0W_0+BSE level of theory, the bright exciton energy being set to 0, in comparison with the conduction band splitting induced by spin-orbit coupling Δ_c. The sign of the e-h exchange contribution is negative. Insets are the corresponding qualitative band structure of the excitons in MoX_2 (left) and WX_2 (right), with bright and dark excitons in red and dotted gray, respectively. (b) Schematics of the one-particle band structure of systems like MoX_2 ML in the K_+ valley; the K_- valley can be obtained by time-reversal symmetry. The spin-orbit induced splittings for valence (Δ_v) and conduction bands (Δ_c) are shown.

Heyd-Scuseria-Ernzerhof (HSE) hybrid functional [50–52] is used as an approximation of the exchange-correlation electronic term, as well as the Perdew-Burke-Ernzerhof (PBE) one [53]. It uses the plane-augmented wave scheme [54,55] to treat core electrons. Fourteen electrons for Mo and W atoms and six for S and Se ones are explicitly included in the valence states. All atoms are allowed to relax with a force convergence criterion below 0.005 eV/Å. After primitive cell relaxation at the PBE level, the optimized lattice parameters, given in Table I, are in good agreement (1%) with previous calculations [56] with all values slightly larger than the bulk experimental ones. A grid of $12 \times 12 \times 1$ k-points has been used, in conjunction with a vacuum height of 17 Å, to take advantage of the error's cancellation in the band-gap estimates [57], and to provide absorption spectra in reasonable agreement with experiments as suggested in different works [13,15]. A Gaussian smearing with a width of 0.05 eV is used for partial occupancies when a tight electronic minimization tolerance of 10^{-8} eV is set to determine with

TABLE I. $\Delta_{B^{ex}-A^{ex}}$: calculated energy splitting between $1s$ A and B bright excitons; $\Delta_{dark-bright}$: calculated dark-bright energy separation for various TMDC MLs of the $1s$ state excitons at the G_0W_0+BSE level using HSE orbitals. The values in parentheses are extracted from G_0W_0-PBE calculations.

Monolayer	$\Delta_{B^{ex}-A^{ex}}$ (eV)		$\Delta_{dark-bright}$ (meV)	
	G_0W_0-HSE	Expt.	A excitons	B excitons
MoS_2	0.18 (0.16)	0.16[a]	0 (−5)	−24 (−20)
$MoSe_2$	0.24 (0.21)	0.22[b]	16 (11)	−45 (−37)
$MoTe_2$	0.33 (0.30)	0.26[c]	34 (25)	−30 (−9)
WS_2	0.45	0.38[d]	−11	−6
WSe_2	0.49	0.43[e]	−16	−37

[a]Reference [62].
[b]Reference [63].
[c]Reference [64].
[d]Reference [65].
[e]Reference [11].

good precision the corresponding derivative of the orbitals with respect to k needed in quasiparticle band structure calculations. Spin-orbit coupling was also included non-self-consistently to determine eigenvalues and wave functions as input for the full-frequency-dependent GW calculations [58] performed at the G_0W_0 level but also at GW_0 level with three iterations of the G term, when necessary. The total number of states included in the GW procedure is set to 600, after a careful check of the direct band-gap convergence, to be smaller than 0.1 eV. All optical excitonic transitions have been calculated by solving the Bethe-Salpeter equation as follows [59,60]:

$$\left(\varepsilon_c^{QP} - \varepsilon_v^{QP}\right)A_{vc} + \sum_{v'c'}\langle vc|K^{eh}|v'c'\rangle A_{v'c'} = \Omega A_{vc}, \qquad (1)$$

where Ω are the resulting e-h excitation energies. A_{vc} are the corresponding eigenvectors, when ε^{QP} are the single-quasiparticle energies obtained at the G_0W_0 level, and K^{eh} being the CB electron-VB hole interaction kernel. This term consists of a first attractive screened direct term and a repulsive exchange part. Practically we have included the six highest valence bands and the eight lowest conduction bands to obtain eigenvalues and oscillator strengths on all systems. Dark excitons are characterized by oscillator strengths around one thousand times smaller than bright ones [61].

Results and discussion. Figure 1(a) and Table I present the calculated values of the splittings $\Delta_{dark-bright}$ between non-optically-active $1s$ exciton transitions $\Omega_{\uparrow\downarrow}$ and active ones $\Omega_{\uparrow\uparrow}$. This splitting is positive for A excitons in the cases of $MoSe_2$ and $MoTe_2$ MLs. These results are compatible with the measured dependence of the photoluminescence (PL) intensity with respect to the temperature [26–29]. If we assume, that the direct contribution terms of the K^{eh} kernel are very close for the two distinct spins orientations for one particular ML, the effect of the e-h exchange term is to partially compensate for the conduction band splitting by subtracting roughly 20 meV for those two systems from Δ_c to obtain the exciton dark-bright splittings, see Figure 1(a). In other words, the CB spin-orbit splitting and the exciton exchange term have opposite signs. Interestingly the exciton exchange contribution seems to be an

invariant quantity for the entire family, at least for the tested TMDC MLs, and agrees well with the single available value of this term in the literature, coming from calculations of a freestanding MoS_2 ML [17]. For the particular $MoSe_2$ and $MoTe_2$ cases, since the conduction band splitting is larger than the exciton exchange term, $\Delta_{\mathrm{dark-bright}}$ is positive, as shown in Figure 1(a). Local-field effects (exciton exchange term) also act on the B exciton, according to the sign change of Δ_c for the transition involving the B valence band series but with almost the same repulsive exchange term, now the $\Omega^B_{\uparrow\downarrow}$ transition appears below the $\Omega^B_{\uparrow\uparrow}$ one. Note that for those two systems, there is also a change in the direct term, since it appears less attractive than in the A case, this is particularly true for $MoTe_2$.

The MoS_2 ML is very intriguing; our calculations show that the CB spin-orbit splitting and the exciton exchange term almost cancel each other yielding very small bright-dark exciton separations. As a consequence, $\Delta_{\mathrm{dark-bright}}$ is negative for PBE-based calculations (-5 meV) and 0 meV when HSE orbitals are used. This is in line with the previous determination of Qiu *et al.* [17] for the same system, since $\Omega^A_{\uparrow\downarrow}$ is lower in energy than $\Omega^A_{\uparrow\uparrow}$ by approximatively 17 meV and $\Omega^B_{\uparrow\downarrow}$ by around 23 meV with respect to $\Omega^B_{\uparrow\uparrow}$. We observe the same trend, the difference being certainly due to our larger Δ_c values obtained at the GW level, see below. On the B exciton, we also observe a small decrease of the direct contribution that makes the absolute energy difference between the parallel and antiparallel spins slightly smaller than the simple addition of the conduction band splitting and the exciton exchange term.

For WS_2 and WSe_2 MLs, since Δ_c is very small in both cases, see Fig. 1(a) and Supplemental Material [66], the exchange term contribution dictates the bright-dark exciton splitting inducing the bright exciton to lie at lower energy compared to the dark one. The corresponding energy separations remain very modest when compared to the binding energy, but at the same time allow one to actively populate the bright excitons when increasing the sample temperature. To be more specific for WSe_2, we propose here an estimate of the dark-bright energy splitting smaller than 20 meV, in good agreement with the indirect determination based on a recent fit procedure of experimental data [28].

The determination of the bright and dark exciton splitting in TMDC MLs requires very high accuracy in the calculations of spin-orbit splitting in the *conduction bands*. It is well documented that standard DFT fails in predicting band structure parameters like band gap or effective masses. Due to the ground-state character of the DFT, conduction band splittings need to be more accurately described by means of many-body based calculations. Here our GW-based calculations provide more accurate band structure parameters compared to standard DFT, as has been shown for similar systems [13,15,56,67]. Here we compare the SOC effects on both valence and conduction bands by means of standard DFT with our results from more advanced GW schemes. All data corresponding to VB energy splittings Δ_v values are reported in the Supplemental Material [66]. Those values agree very well with previous DFT-based reports [33,38,39,56]. It clearly shows that adding a partial exact exchange contribution to the electronic exchange-correlation functional significantly enlarges Δ_v for all TMDC MLs. This trend is directly observable

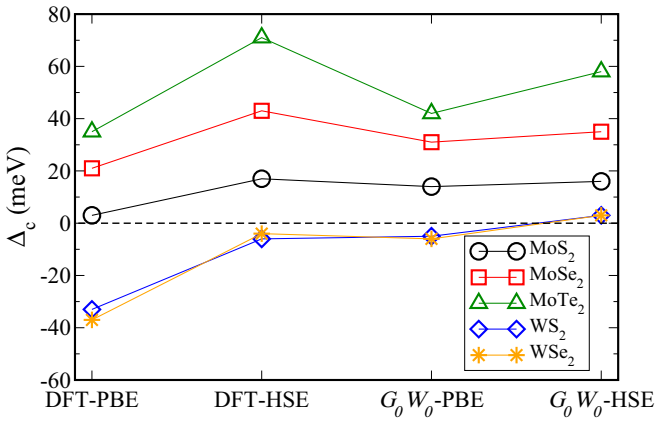

FIG. 2. Evolution of the calculated conduction band splittings with respect to the level of theory for five TMDC monolayers. The data are extracted from Table SI-1 in [66].

in the computed absorption spectra and more specifically in the $\Delta_{B^{ex}-A^{ex}}$ results of Table I which include contributions both from Δ_v and Δ_c but also e-h interaction effects. HSE-based calculations always give larger A-B splittings than the experimental estimates, but still remain in a reasonable agreement with them. Considering Δ_c, at the DFT level, our results are similar to previous reports [33,39]: for the MoX_2 family, when going from a semilocal to a hybrid approximation of the electronic exchange-correlation term, the splittings between spin-↑ and ↓ CB states are enhanced, see Fig. 2 and Supplemental Material [66]. Interestingly for the WS_2 and WSe_2 cases, if now ↓ CB is the lowest unoccupied state, the energy separation is significantly reduced in hybrid functional calculations, meaning that short-range Hartree-Fock terms strongly influence atomic SOC contributions from both the transition metal and the chalcogen, to make them competitive with opposite signs [33]. For the MoS_2 and $MoSe_2$ cases, our G_0W_0 calculations based on PBE or HSE wave functions provide similar Δ_c splittings suggesting a nondependence band splitting on the ground-state orbitals in contrast with $MoTe_2$ ML, probably due to an overestimation of the chalcogen contribution using HSE-based orbitals, which leaves Δ_c 40% larger even after applying a single shot GW correction. Remarkably for W-based systems, the GW scheme reduces drastically Δ_c starting from PBE orbitals, and even reverses again the spin-up and spin-down conduction band ordering in HSE-based calculations. This clearly indicates that ↑ and ↓ CB states are almost degenerate at the GW level, contrary to standard DFT predictions.

The G_0W_0 results reveal further interesting details: as it has been already reported [56] and mentioned in the present Rapid Communication, all the extracted values of GW calculations, namely, Δ_v, Δ_c, and E_g (free carrier gap value) are sensitive to the choice of the starting set of orbitals. Larger values of E_g are yielded and a better agreement with previous calculations of the exciton binding energies are obtained when HSE wave functions are used, as shown in the Supplemental Material [66]. Unexpectedly, PBE-based calculations give an indirect band gap in K_+-Λ, with values smaller by 0.03 and 0.05 eV respectively when compared to direct K_+-K_+ gaps for WS_2 and WSe_2. However, these surprising results

agree with a recent experimental result [68]. The choice of lattice parameter value is also important for the resulting band structure properties: using the experimental lattice parameter results in different values for Δ_c mainly. Preeminently most of the systems have an indirect band gap with this particular choice of the lattice parameter [66], even after the use of the partially self-consistent GW_0 scheme. This supports us in our particular choices of exchange-correlation functional (HSE) at the DFT level and of the lattice parameter values (optimized ones), for which all MLs have direct band gaps in good agreement with previous studies.

Conclusions. Our calculations demonstrate that the bright to dark exciton energy splitting in MoX_2 and WX_2 monolayers depends in both sign and amplitude on the electron-hole short-range Coulomb exchange within the exciton. In addition to this exchange energy, the conduction band spin-orbit splitting Δ_c needs to be taken into account, which has initially been put forward as the main origin of the dark-bright exciton splitting. To measure the splitting between Δ_c between electron spin states in the absence of holes, techniques like angle-resolved photoemission spectroscopy (ARPES) [69] or electron spin resonance would be desirable, because pure optical spectroscopy techniques (absorption, emission) cannot separate this contribution from the strong electron-hole Coulomb exchange effects.

Acknowledgments. We thank Misha Glazov for fruitful discussions and ANR MoS2ValleyControl and Programme Investissements d'Avenir ANR-11-IDEX-0002-02, reference ANR-10-LABX-0037-NEXT for financial support. The authors also acknowledge the CALMIP initiative for the generous allocation of computational times, through Project p0812, as well as the GENCI-CINES, GENCI-IDRIS, and GENCI-CCRT for Grant No. x2015096649. I.C.G. also thanks the CNRS for his financial support. X.M. acknowledges the Institut Universitaire de France. B.U. is supported by ERC Grant No. 306719.

[1] K. F. Mak, C. Lee, J. Hone, J. Shan, and T. F. Heinz, Phys. Rev. Lett. **105**, 136805 (2010).

[2] A. Splendiani, L. Sun, Y. Zhang, T. Li, J. Kim, C.-Y. Chim, G. Galli, and F. Wang, Nano Lett. **10**, 1271 (2010).

[3] T. Cao, G. Wang, W. Han, H. Ye, C. Zhu, J. Shi, Q. Niu, P. Tan, E. Wang, B. Liu *et al.*, Nat. Commun. **3**, 887 (2012).

[4] H. Zeng, J. Dai, W. Yao, D. Xiao, and X. Cui, Nat. Nanotechnol. **7**, 490 (2012).

[5] K. F. Mak, K. He, J. Shan, and T. F. Heinz, Nat. Nanotechnol. **7**, 494 (2012).

[6] G. Sallen, L. Bouet, X. Marie, G. Wang, C. R. Zhu, W. P. Han, Y. Lu, P. H. Tan, T. Amand, B. L. Liu *et al.*, Phys. Rev. B **86**, 081301 (2012).

[7] D. Xiao, G.-B. Liu, W. Feng, X. Xu, and W. Yao, Phys. Rev. Lett. **108**, 196802 (2012).

[8] A. Chernikov, T. C. Berkelbach, H. M. Hill, A. Rigosi, Y. Li, O. B. Aslan, D. R. Reichman, M. S. Hybertsen, and T. F. Heinz, Phys. Rev. Lett. **113**, 076802 (2014).

[9] Z. Ye, T. Cao, K. O'Brien, H. Zhu, X. Yin, Y. Wang, S. G. Louie, and X. Zhang, Nature **513**, 214 (2014).

[10] K. He, N. Kumar, L. Zhao, Z. Wang, K. F. Mak, H. Zhao, and J. Shan, Phys. Rev. Lett. **113**, 026803 (2014).

[11] G. Wang, X. Marie, I. Gerber, T. Amand, D. Lagarde, L. Bouet, M. Vidal, A. Balocchi, and B. Urbaszek, Phys. Rev. Lett. **114**, 097403 (2015).

[12] D. Y. Qiu, F. H. da Jornada, and S. G. Louie, Phys. Rev. Lett. **111**, 216805 (2013).

[13] A. Molina-Sánchez, D. Sangalli, K. Hummer, A. Marini, and L. Wirtz, Phys. Rev. B **88**, 045412 (2013).

[14] M. M. Ugeda, A. J. Bradley, S.-F. Shi, F. H. da Jornada, Y. Zhang, D. Y. Qiu, W. Ruan, S.-K. Mo, Z. Hussain, Z.-X. Shen *et al.*, Nat. Mater. **13**, 1091 (2014).

[15] A. R. Klots, A. K. M. Newaz, B. Wang, D. Prasai, H. Krzyzanowska, J. Lin, D. Caudel, N. J. Ghimire, J. Yan, B. L. Ivanov *et al.*, Sci. Rep. **4**, 6608 (2014).

[16] D. Y. Qiu, F. H. da Jornada, and S. G. Louie, Phys. Rev. Lett. **115**, 119901(E) (2015).

[17] D. Y. Qiu, T. Cao, and S. G. Louie, Phys. Rev. Lett. **115**, 176801 (2015).

[18] Here we work in the electron formalism (not hole), where the conduction electron has the same spin as the valence state it occupied before. Same spin transitions are therefore optically allowed.

[19] E. Blackwood, M. J. Snelling, R. T. Harley, S. R. Andrews, and C. T. B. Foxon, Phys. Rev. B **50**, 14246 (1994).

[20] J. Puls and F. Henneberger, Phys. Status Solidi A **164**, 499 (1997).

[21] T. Amand, X. Marie, P. Le Jeune, M. Brousseau, D. Robart, J. Barrau, and R. Planel, Phys. Rev. Lett. **78**, 1355 (1997).

[22] L. Besombes, K. Kheng, D. Martrou, N. Magnea, and T. Charvolin, Phys. Status Solidi A **178**, 197 (2000).

[23] E. Vanelle, M. Paillard, X. Marie, T. Amand, P. Gilliot, D. Brinkmann, R. Lévy, J. Cibert, and S. Tatarenko, Phys. Rev. B **62**, 2696 (2000).

[24] S. A. Crooker, T. Barrick, J. A. Hollingsworth, and V. I. Klimov, Appl. Phys. Lett. **82**, 2793 (2003).

[25] A. Arora, M. Koperski, K. Nogajewski, J. Marcus, C. Faugeras, and M. Potemski, Nanoscale **7**, 10421 (2015).

[26] A. Arora, K. Nogajewski, M. Molas, M. Koperski, and M. Potemski, Nanoscale **7**, 20769 (2015).

[27] G. Wang, C. Robert, A. Suslu, B. Chen, S. Yang, S. Alamdari, I. C. Gerber, T. Amand, X. Marie, S. Tongay *et al.*, Nat. Commun. **6**, 10110 (2015).

[28] X.-X. Zhang, Y. You, Shu Yang Frank Zhao, and T. F. Heinz, Phys. Rev. Lett. **115**, 257403 (2015).

[29] F. Withers, O. Del Pozo-Zamudio, S. Schwarz, S. Dufferwiel, P. M. Walker, T. Godde, A. P. Rooney, A. Gholinia, C. R. Woods, P. Blake *et al.*, Nano Lett. **15**, 8223 (2015).

[30] S. Wu, S. Buckley, J. R. Schaibley, L. Feng, J. Yan, D. G. Mandrus, F. Hatami, W. Yao, J. Vučković, A. Majumdar *et al.*, Nature **520**, 69 (2015).

[31] Y. Ye, Z. J. Wong, X. Lu, X. Ni, H. Zhu, X. Chen, Y. Wang, and X. Zhang, Nat. Photon. **9**, 733 (2015).

[32] M. Combescot, O. Betbeder-Matibet, and R. Combescot, Phys. Rev. Lett. **99**, 176403 (2007).

[33] K. Kośmider, J. W. González, and J. Fernández-Rossier, Phys. Rev. B **88**, 245436 (2013).
[34] G.-B. Liu, W.-Y. Shan, Y. Yao, W. Yao, and D. Xiao, Phys. Rev. B **88**, 085433 (2013).
[35] A. Kormanyos, G. Burkard, M. Gmitra, J. Fabian, V. Zolyomi, N. D. Drummond, and V. Fal'ko, 2D Mater. **2**, 022001 (2015).
[36] H. Dery and Y. Song, Phys. Rev. B **92**, 125431 (2015).
[37] Z. Y. Zhu, Y. C. Cheng, and U. Schwingenschlögl, Phys. Rev. B **84**, 153402 (2011).
[38] T. Cheiwchanchamnangij, W. R. L. Lambrecht, Y. Song, and H. Dery, Phys. Rev. B **88**, 155404 (2013).
[39] K. Kośmider and J. Fernández-Rossier, Phys. Rev. B **87**, 075451 (2013).
[40] R. Roldán, J. A. Silva-Guillén, M. P. López-Sancho, F. Guinea, E. Cappelluti, and P. Ordejón, Ann. Phys. (NY) **526**, 347 (2014).
[41] B. R. Salmassi and G. E. W. Bauer, Phys. Rev. B **39**, 1970 (1989).
[42] H. Yu, G.-B. Liu, P. Gong, X. Xu, and W. Yao, Nat. Commun. **5**, 3878 (2014).
[43] C. R. Zhu, K. Zhang, M. Glazov, B. Urbaszek, T. Amand, Z. W. Ji, B. L. Liu, and X. Marie, Phys. Rev. B **90**, 161302 (2014).
[44] M. M. Glazov, E. L. Ivchenko, G. Wang, T. Amand, X. Marie, B. Urbaszek, and B. L. Liu, Phys. Status Solidi B **252**, 2349 (2015).
[45] T. Yu and M. W. Wu, Phys. Rev. B **89**, 205303 (2014).
[46] L. Hedin, Phys. Rev. **139**, A796 (1965).
[47] F. Aryasetiawan and O. Gunnarsson, Rep. Prog. Phys. **61**, 237 (1998).
[48] G. Kresse and J. Hafner, Phys. Rev. B **47**, 558(R) (1993).
[49] G. Kresse and J. Furthmüller, Phys. Rev. B **54**, 11169 (1996).
[50] J. Heyd and G. E. Scuseria, J. Chem. Phys. **120**, 7274 (2004).
[51] J. Heyd, J. E. Peralta, G. E. Scuseria, and R. L. Martin, J. Chem. Phys. **123**, 174101 (2005).
[52] J. Paier, M. Marsman, K. Hummer, G. Kresse, I. C. Gerber, and J. G. Ángyán, J. Chem. Phys. **124**, 154709 (2006).
[53] J. P. Perdew, K. Burke, and M. Ernzerhof, Phys. Rev. Lett. **77**, 3865 (1996).
[54] P. E. Blöchl, Phys. Rev. B **50**, 17953 (1994).
[55] G. Kresse and D. Joubert, Phys. Rev. B **59**, 1758 (1999).
[56] A. Ramasubramaniam, Phys. Rev. B **86**, 115409 (2012).
[57] F. Hüser, T. Olsen, and K. S. Thygesen, Phys. Rev. B **88**, 245309 (2013).
[58] M. Shishkin and G. Kresse, Phys. Rev. B **74**, 035101 (2006).
[59] W. Hanke and L. J. Sham, Phys. Rev. Lett. **43**, 387 (1979).
[60] M. Rohlfing and S. G. Louie, Phys. Rev. Lett. **81**, 2312 (1998).
[61] It turns out from group theory that the A excitons termed dark here are in fact slightly allowed for Z modes of light propagating along the plane of the layer, while B excitons termed dark are strictly forbidden (see on-line Supplemental Material for more details).
[62] K. F. Mak, K. He, C. Lee, G. H. Lee, J. Hone, T. F. Heinz, and J. Shan, Nat. Mater. **12**, 207 (2012).
[63] G. Wang, I. C. Gerber, L. Bouet, D. Lagarde, A. Balocchi, M. Vidal, T. Amand, X. Marie, and B. Urbaszek, 2D Mater. **2**, 1 (2015).
[64] C. Ruppert, O. B. Aslan, and T. F. Heinz, Nano Lett. **14**, 6231 (2014).
[65] B. Zhu, X. Chen, and X. Cui, Sci. Rep. **5**, 9218 (2015).
[66] See Supplemental Material at http://link.aps.org/supplemental/10.1103/PhysRevB.93.121107, which includes detailed tables for the valence and conduction band splittings, as well as free carrier band-gap results and extracted binding energies of the A 1s states. Dark-bright splittings on B excitons are also depicted and a symmetry analysis of exciton symmetry is presented.
[67] H. L. Zhuang and R. G. Hennig, Chem. Mater. **25**, 3232 (2013).
[68] C. Zhang, Y. Chen, A. Johnson, M.-Y. Li, L.-J. Li, P. C. Mende, R. M. Feenstra, and C.-K. Shih, Nano Lett. **15**, 6494 (2015).
[69] Y. Zhang, T.-R. Chang, B. Zhou, Y.-T. Cui, H. Yan, Z. Liu, F. Schmitt, J. Lee, R. Moore, Y. Chen *et al.*, Nat. Nanotechnol. **9**, 111 (2014).